ECE 445

SENIOR DESIGN LABORATORY

FINAL REPORT

Electromagnetic Launch System with Switchblade Drone : Final Report for ECE 445

Team #4

SHUYANG QIAN (sq8@illinois.edu)
ZHENG FANG (zhengf4@illinois.edu)
XINYU XIA (xinyux4@illinois.edu)
RUIKE YAN (ruikey2@illinois.edu)

TA: Adeel Ahmed

May 22, 2023

Abstract

The increasing use of Unmanned Aerial Vehicles (UAVs) across various industries calls for a thorough understanding of their societal implications. This paper discusses an ideal launching solution for drone which is promising in both launching speed, portability, and cost. To achieve these prospects, we propose a novel solution: an electromagnetic launch system and a drone design with switchable wings. We wish our system to be able to effectively deploy Switchblade drones for a wide range of commercial applications. Four subsystems are included: power supply subsystem, electromagnetic accelerator subsystem, switchblade drone subsystem and flight control subsystem.

Keywords: Unmanned Aerial Vehicles (UAVs), Switchblade UAVs, Electromagnetic Launch System, Electromagnetic Acceleration, Drone Technology.

Contents

1 Introduction

1.1 Purpose

In modern society, the widespread adoption of Unmanned Aerial Vehicles (UAVs) [1] has introduced a plethora of benefits and opportunities. However, with these advancements come new challenges and concerns that need to be addressed. The rapid proliferation of UAVs in various sectors, such as agriculture, disaster management, surveillance, delivery services, and environmental monitoring, highlights the need for a comprehensive understanding of the implications of this technology on society.

Switchblade UAVs are small but highly effective drones that have gained popularity in commercial applications due to their maneuverability, versatility, and ability to be launched quickly and quietly. However, the current technology used to power these drones, pneumatics, has limitations in terms of launching speed, cost, and portability. Additionally, the existing Switchblade UAVs require computer chips to control the UAV to spread the wings of the drone. This process can be time-consuming and may lead to delays in operations. To overcome these challenges and improve the design of Switchblade UAVs, there is a need to explore alternative power sources. To successfully develop this technology, it is essential to draw upon expertise from both commercial and engineering sectors. Commercial experts can provide valuable insights into the specific requirements of UAVs in various industries, while engineering experts can help ensure that the technology is scalable, cost-effective, and technically viable. By bringing together expertise from multiple fields, it may be possible to develop an electromagnetic launch system that revolutionizes the field of drone technology.

In recent years, there has been a growing interest in electromagnetic technology as a means of powering drones [2]. This technology offers several advantages over traditional power sources, including faster launching speeds, greater portability, and reduced costs. By harnessing the power of electromagnetism, it may be possible to improve the design of Switchblade UAVs and make them more effective in commercial applications, such as aerial photography, inspections, agriculture, and delivery services.

1.2 Functionality

The project's primary objective is to develop an electromagnetic launch system that effectively launches Switchblade drones for diverse commercial applications. This innovative solution for high-speed unmanned aerial vehicles incorporates the latest advances in electromagnetic technology, using high-powered magnets and electromagnetic coils to provide a powerful and efficient launch mechanism [3]. The resulting system will be lightweight, portable, and easy to deploy.

The project's high-level functionalities and their relation to the overall purpose are:

1. The drone must accelerate continuously, achieving a take-off speed of 1-3 m/s. The

launch system should operate with a dip angle of 0-30 degrees and function outdoors under wind speeds of 0-3 m/s. This functionality ensures a reliable launch system that can adapt to various environmental conditions.

2. The Switchblade drone should fold its wings on the launch rail and complete the deployment of all four wings within 1 second after launch. This functionality allows for a compact form factor during launch, which reduces drag and increases the drone's aerodynamic efficiency upon wing deployment.

3. The drone should be capable of flying a distance of 10 meters after launch. This functionality demonstrates the launch system's effectiveness in propelling the drone and achieving the necessary flight performance for various commercial applications.

To achieve a functioning system, the project focuses on four critical steps: design and construction of the launch system, development of the foldable wing mechanism, integration of subsystems, and testing and validation.

Electromagnetic-launched drones offer advantages over pneumatic-launched drones, as they do not require heavy air pumps. Instead, they can use convenient batteries or capacitors, reducing the overall weight and making the system more portable and user-friendly.

Furthermore, existing drones often consist of metal, which can be heavy and expensive. In contrast, lightweight polylactic acid (PLA) materials can be used for Switchblade drones, offering a lower cost and lighter mass. This design suits the disposable nature of the Switchblade drone, making it more cost-effective and versatile for commercial usage.

Through careful planning, design, and testing, this project has the potential to revolutionize the field of unmanned aerial vehicles, enabling high-speed, long-distance flights with a Switchblade drone that is lightweight, cost-effective, and more suitable for various commercial applications.

1.3 Subsystem Overview

The whole system is separated into four subsystems: power supply, electromagnetic accelerator, switchblade drone and flight control. Figure 1 shows the block diagram for the entire system, including the four subsystems and their connections.

1.3.1 Block Diagram

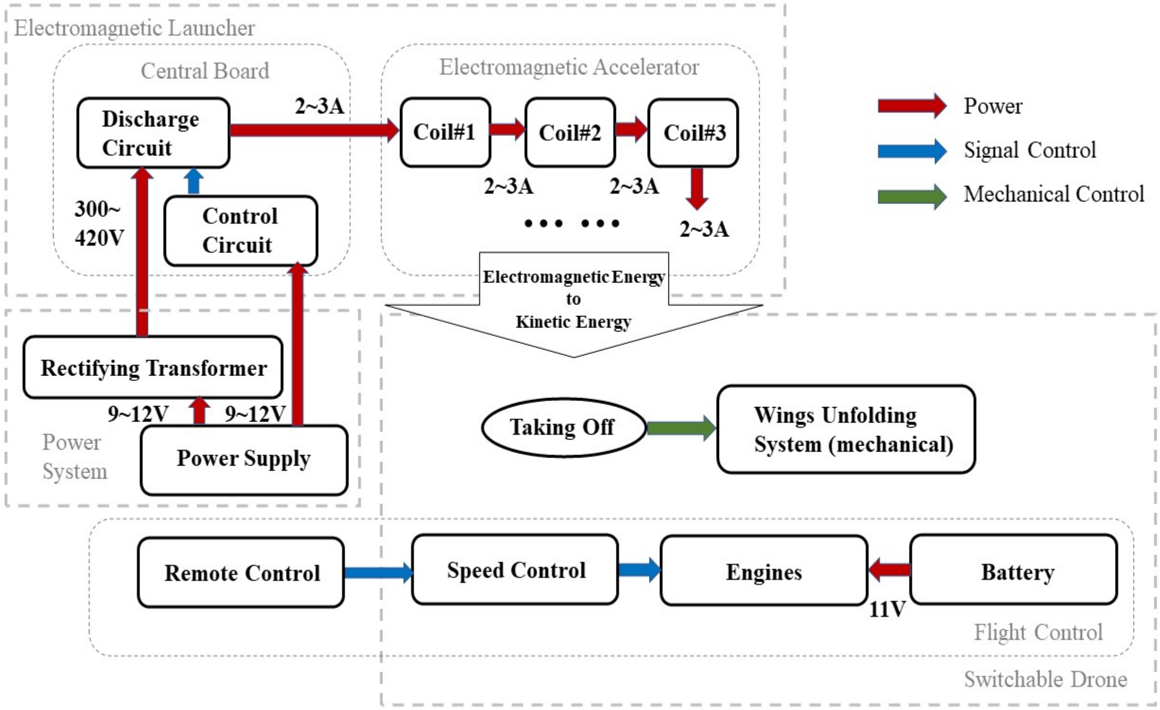

Figure 1: Block Diagram

1.3.2 Power Supply Subsystem

The Electromagnetic Launch System for drones comprises a power supply subsystem that is responsible for converting a wide range of input voltage (9 V to 12 V) into a regulated 450 V DC output voltage. This subsystem is crucial for drone launch system reliability and safety. The power supply system is directly connected to the charge circuit unit of the electromagnetic accelerator subsystem. This provides enough power to generate a strong magnetic field. The power supply subsystem consists of several stages: input filtering, rectification, a Zero Voltage Switching (ZVS) resonant converter, output rectification, voltage regulation, and circuit protection.

In addition to these stages, 6 capacitors with 450 V and 1500 μF are used to store energy, providing instantaneous burst energy for drone acceleration and preventing circuit damage. The materials used for fixing the coils and components are resistant to high voltage and high temperature.

1.3.3 Electromagnetic Accelerator Subsystem

There are two modules in electromagnetic accelerator subsystem: a central board module and a mechanical structure module. The electromagnetic launch subsystem is designed to accelerate a cart, which is attached to a drone and two iron blocks, using electromagnetic forces. This subsystem leverages the principles of electromagnetic induction and interaction between magnetic fields to propel the drone along a launch track.

1.3.4 Switchblade Drone Subsystem

This subsystem consists of the main body and two sets of flexible wings. The main body provides a stable platform for the flexible wings and the fly control subsystem. The main body is 3D printed using light PLA material. The flexible wings mechanism is achieved through mechanical structure. It opens the wings after the drone leave the electronic launcher. After the wing is open, the structure is fixed and ensure the wing cannot move during the flying process. The subsystem can also fold the wing inside the main body when the drone is inside the launcher. This function is achieved by a spring system. When the slider is connected to the drone (the drone is inside the launcher) the slider will press the spring and fold the wing inside the body. After the pressure is removed, the spring recover to its initial position to open the wing. After the wing is open the fix structure will fix the wing. The total length of the drone is 248 mm, and the width is 108mm. The length of the wings is 150 mm, and the width is 40 mm. The total weight of the drone is about 400 g.

1.3.5 Flight Control Subsystem

The flight control subsystem enables the drone to be able to navigate a certain distance after taking off. The flight control system provides thrust during the fly and helps the drone to turn its direction. This subsystem is closely related to other subsystems and serves as a important part of the greater project. The power needed for flight control is largely decided by the weight and shape of the switchable drone, along with the final velocity the electromagnetic launcher can give to the drone. The size and weight limitation of the flight control subsystem is also decided by the characteristics of the drone and the performance of the electromagnetic accelerator. By carefully collecting and analyzing data of our drone and launcher, our goal is to build a flight control system that best suits our project.

2 Design

2.1 Power Supply Subsystem

2.1.1 Design Description & Justification

We designed our DC power supply subsystem strictly based on commercial ZVS boost modules which were portable and safe. The subsystem interconnects can be summarized as follows:

1. **Input Stage (Electromagnetic Interference Filter):** An Electromagnetic Interference (EMI) filter is used to minimize noise and interference from the input voltage, thereby improving the system's power quality.

2. **Rectification Stage:** The input voltage is rectified and filtered using a full-bridge rectifier and capacitor filter, providing a constant DC voltage for the ZVS resonant converter.

3. **ZVS Resonant Converter:** The core of the power supply subsystem, is responsible for stepping up the rectified DC voltage to the required 450 V output voltage. The ZVS converter utilizes a high-frequency transformer, resonant inductor, resonant capacitor, and switching devices such as metal oxide semiconductor field-effect transistors (MOSFETs) to achieve zero-voltage switching, resulting in improved efficiency.

4. **Output Rectification Stage:** The output of the ZVS converter is rectified and filtered using Schottky diodes and a capacitor filter to produce a stable 450 V DC output voltage.

5. **Voltage Regulation:** A feedback loop, incorporating an optocoupler for isolation and a voltage reference, is used to maintain a consistent output voltage of 450V, regardless of load changes.

6. **Circuit Protection:** Various protection measures, such as fuses, overvoltage protection, and reverse polarity protection, are integrated to safeguard the subsystem from potential hazards.

7. **Safety Considerations:** Proper grounding, isolation between AC and DC sides, and thermal management through adequate heat sinking and ventilation are addressed to ensure reliable operation and user safety.

The circuit diagram of the entire subsystem is shown in Figure 2. It works by rapidly switching MOSFETs on and off, creating a fluctuating magnetic field within a transformer's ferrite core. This action induces a high voltage in the secondary coil due to the large number of windings. The ZVS oscillator operates by leveraging a resonant tank circuit, formed by a capacitor in parallel with the coil, which ensures efficient switching and minimizes losses.

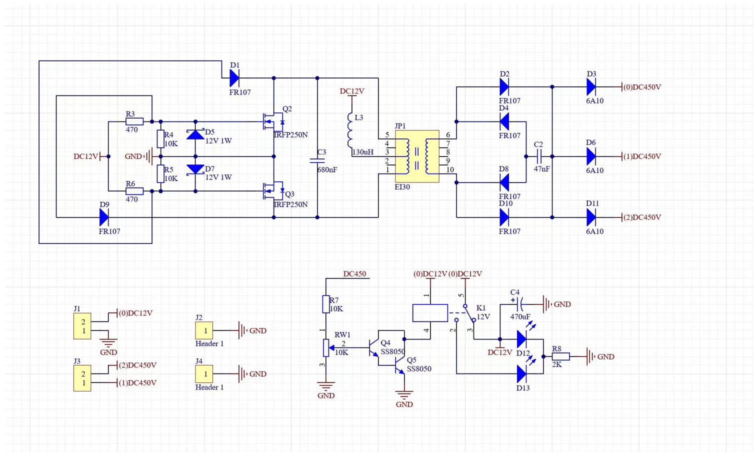

Figure 2: Circuit Design Diagram

We also did some mathematical calculations to ensure safety and feasibility. We assume the efficiency of the power supply module is $\phi = 60\%$ and the power we need is 100 W. Equation 1 and 2 show the max and min input voltage. Equation 3 calculates the expected input power. Based on equation 1, 2 and 3, equation 4 and 5 show the max and min input current.

$$V_{inMin} = 9 \text{ V} \tag{1}$$

$$V_{inMax} = 12 \text{ V} \tag{2}$$

$$P = \frac{P_{out}}{\phi} = \frac{100 \text{ W}}{0.6} = 166.667 \text{ W} \tag{3}$$

$$I_{inMin} = \frac{P}{V_{inMin}} = \frac{1666.67 \text{ W}}{9 \text{ V}} = 18.519 \text{ A} \tag{4}$$

$$I_{in_max} = \frac{P}{V_{inMax}} = \frac{1666.67 \text{ W}}{12 \text{ V}} = 13.889 \text{ A} \tag{5}$$

2.1.2 Design Alternatives

There were two major issues with the initial design solution. We have proposed improvements for these two issues and built this subsystem. The completed ZVS module is shown in Figure 3.

1. The input voltage requirements for the subsystem are stringent, necessitating near-constant voltage and current to energize it and charge the capacitor. During actual testing, laboratory constant current or constant voltage sources may not meet the specified voltage or current levels. This can lead to an output voltage or current exceeding the circuit's tolerable limits, resulting in the entire module burning out.

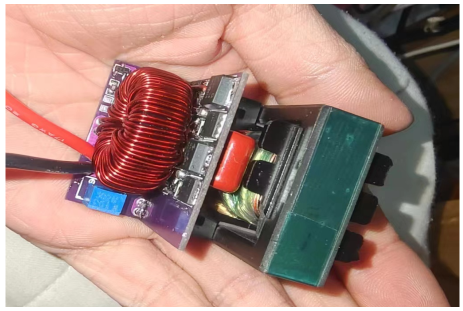

Figure 3: Physical Photo for Power Supply

Given that the complete launch system is intended for outdoor use, we have adapted our input source to incorporate three rechargeable and dischargeable batteries. This solution satisfies the module's input requirements while also offering convenience and portability to the system.

2. For the output voltage that is not stable at 450 V, we can hardly judge whether the voltage we need is reached.

   A readable voltmeter is connected in parallel to the output of the ZVS booster module to allow us to easily read and adjust the output voltage.

2.2 Electromagnetic Accelerator Subsystem

2.2.1 Design Description & Justification

The central board module is a self-halting charging circuit, which is regulated by a relay. This charging circuit is responsible for energizing three distinct sets of capacitors.

To safeguard against any potential backflow of current, diodes have been strategically connected to these capacitors. Furthermore, these capacitors are interconnected via photoresistances, forming an innovative system that leverages the properties of light. A specially designed cart is utilized to intermittently obstruct the passage of light to these photoresistances. This intervention serves to facilitate a sequential, stage-by-stage acceleration process.

Additionally, photoresistances have been linked to thyristors, often referred to as silicon-controlled rectifiers in the field. These components play a pivotal role in the regulation of the capacitors' charge and discharge cycles.The primary components incorporated in this novel design are as follows:

1. **Relay**: Tasked with controlling the self-halting charging circuit.
2. **Capacitors**: Three distinct sets, energized by the relay-regulated circuit.
3. **Diodes**: Connected to the capacitors, serving to prevent undesirable current backflow.

4. **Photoresistances**: Facilitate interconnection between capacitors and assist in the stage-by-stage acceleration process by responding to changes in light.

5. **Thyristors (Silicon-Controlled Rectifiers)**: Connected to the photoresistances, managing the charging and discharging cycles of the capacitors.

The circuit diagram is shown in Figure 4.

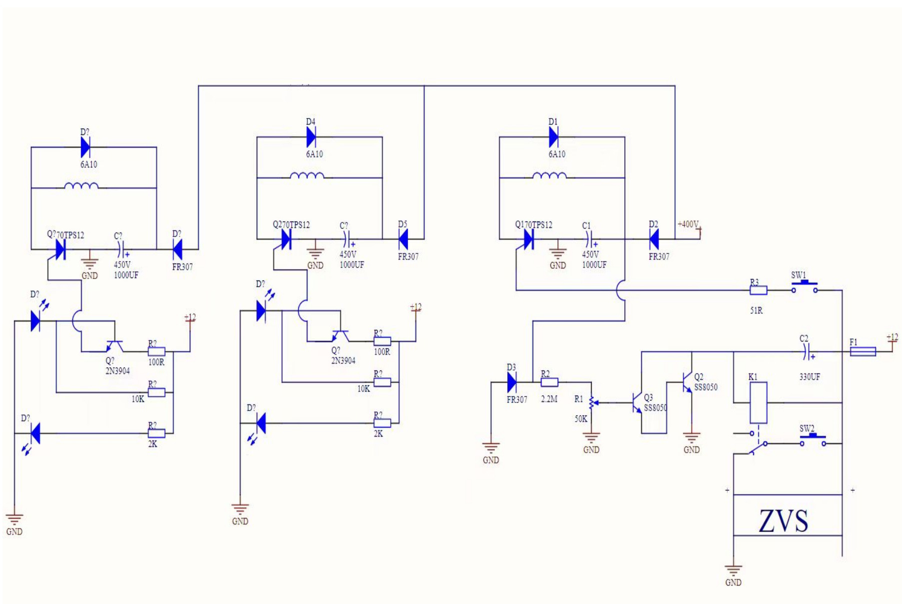

Figure 4: Circuit Design Diagram

According to Xin's research [4], when the voltage is 450 V and the capacity is 1000 μF, the energy conversion efficiency is about 0.04.

$$C = 1000\ \mu\text{F} \tag{6}$$

$$U = 450\ \text{V} \tag{7}$$

$$E = \frac{1}{2}CU^2 = 101.25\ \text{J} \tag{8}$$

$$\eta = 0.04 \tag{9}$$

$$E_{total} = 6\eta E = 24.3\ \text{J} \tag{10}$$

$$m = 1\ \text{kg} \tag{11}$$

$$v = 6\ \text{m/s} \tag{12}$$

$$E_k = \frac{1}{2}mv^2 = 18 \text{ J} \tag{13}$$

$$E_{total} > E_k \tag{14}$$

Equation 6, 7 and 8 show the energy of one capacity stored. Equation 9 shows the energy conversion efficiency. Equation 10 shows the total energy which six coils can convert to kinematic energy. Equation 11, 12, and 13 show the desired kinematic energy for cart and drone. Euqation 14 shows that 6 sets of coils are a reasonable design to accelerate the drone to 6 m/s.

The mechanical structure module is needed to let the cart which connects with iron blocks and drone accelerates continuously in a fixed direction. The mechanical design is based on the function of central board module. And we need following key components:

1. **Linear Guideway**: Linear guideway is a standard guideway which has fixed dimensions. It fits perfectly as the rail of the launch system for the reason that it is easy to design related non-standard parts such as cart. Additionally, it has a relatively low friction coefficient, which is conducive to improving the launch speed. The diagrams are shown in Figure 5.

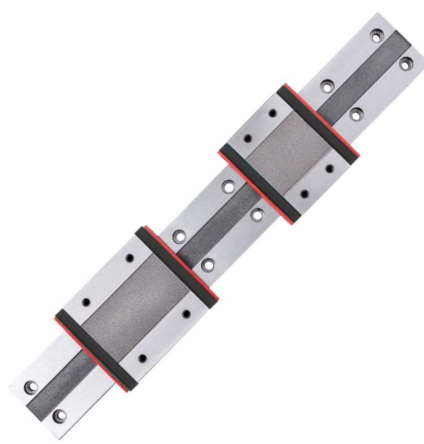

Figure 5: Linear Guideway Diagram

2. **Side Plates and Bottom Plates**: Side plates and bottom plates are designed to fix the linear guideway, coils and photoresistances. There are M3 holes on bottom plates which fit the dimension of linear guideway in order to fix it in the desired direction. There are two different kinds of side plates. One of them is to fix the coils and photoresistances. There are holes prepared to stick the coils and photoresistances. The other kind is to limit the position of the drone's wings. When the drone leaves the range of the side plates, the wings will deploy automatically. The system diagram is shown in Figure 6.

3. **Cart**: The cart should be fixed with iron blocks and drone. The iron blocks should be parallel with coil so that it can be accelerated by electromagnetic force. The drone should be fixed with the drone but separates after the cart arrives at the end of the rail. Additionally, the cart should slide in the gap of the rail. The cart should be also able to trigger the photoresistance when it passes through the previous coil. The CAD diagram is shown in Figure 7.

Overall, the electromagnetic launch subsystem provides a rapid and controlled means of accelerating a drone by exploiting the interactions between magnetic fields and moving charges. This technology can offer significant advantages in terms of efficiency, scalability, and the potential for non-contact propulsion, making it a promising option for various applications, including drone launching systems.

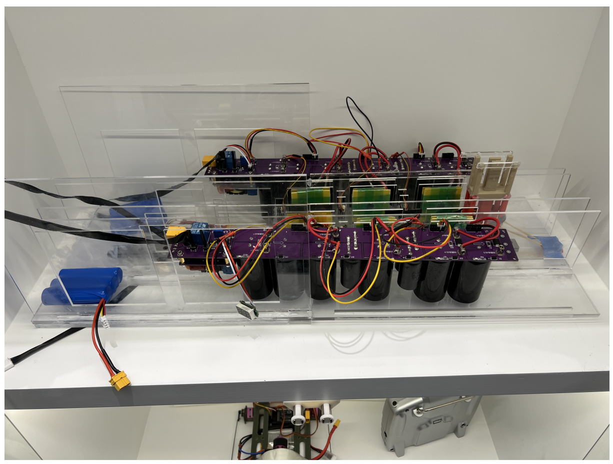

Figure 6: System Overview

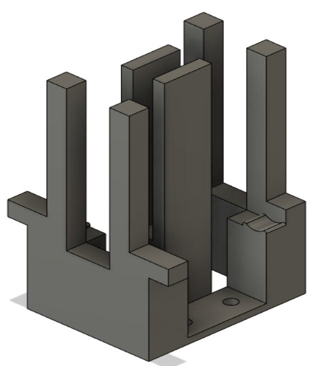

Figure 7: Design of Cart

2.2.2 Design Alternatives

For the central board module, photoresistances are utilized to replace hall effect sensor. In the test, it was found that the frictional force and other non-vertical forces often resulted in occasional displacement of the cart.This displacement interfered with the sensor's ability to consistently detect the cart's movement, which in turn led to inconsistencies in the staged acceleration process. The use of photoresistances not only circumvents the aforementioned issue of cart displacement but also provides a robust and reliable alternative for monitoring the cart's motion and controlling the sequential acceleration. This revised approach promises to enhance the overall performance and reliability of our electromagnetic launch system.

For the mechanical structure module, there were three major issues with the initial design solution. According to these issues, we have built the subsystem. The completed electromagnetic accelerator system is shown in Figure 6.

1. The object being accelerated by the magnetic field is replaced by an iron block instead of a magnet. Although in theory the magnet could be accelerated faster, in practical experiments it was found that the magnet would spin itself and easily fall out of the cart.

2. Using linear guideway instead of 4080 aluminum, the cart can be fixed on track better and have less friction. At the same time, it reduces the weight of the entire launch system, making it easier to carry.

3. The cart's design has changed completely. The new cart has a higher height because the drone needs to avoid collision with the circuit. At the same time, it needs to trigger the photoresistances as it moves forward.

2.3 Switchblade Drone Subsystem

2.3.1 Design Description & Justification

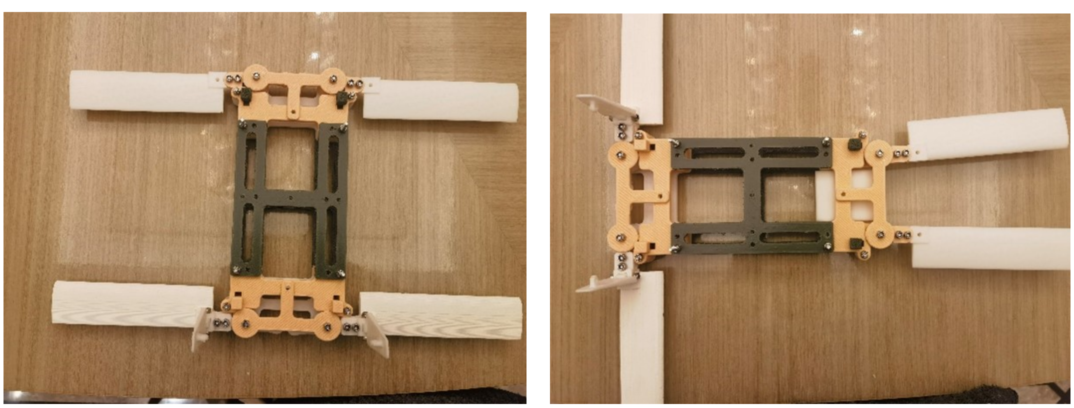

(a) Switchblade Drone (Open)　　(b) Switchblade Drone (Fold)

Figure 8: Overview of the Switchblade Drone

Figure 8(a) and 8(b) shows the switchblade drone. The switchblade drone mainly consists of the following parts:

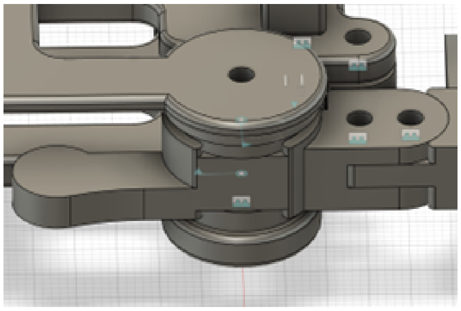

(a) Switchblade Structure (Open)

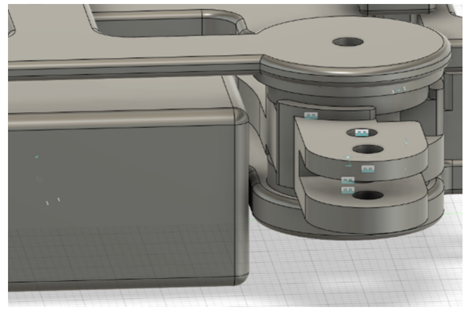

(b) Switchblade Structure (Fold)

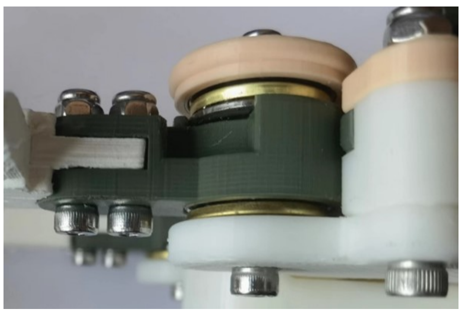

(c) Switchblade Structure (Open)

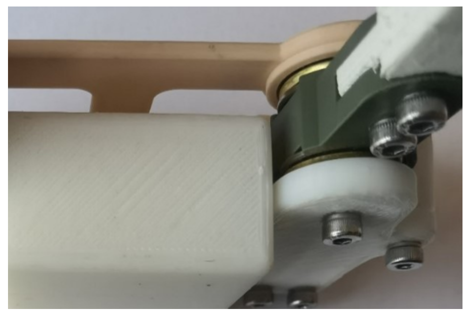

(d) Switchblade Structure (Fold)

Figure 9: Switchblade Structure

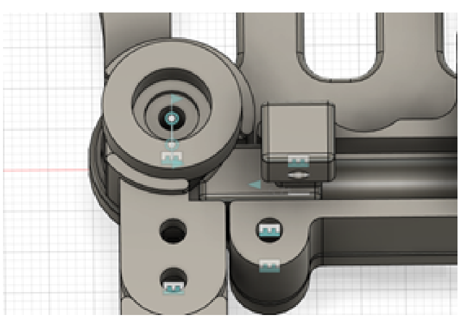

(a) Locking Mechanism (Lock)

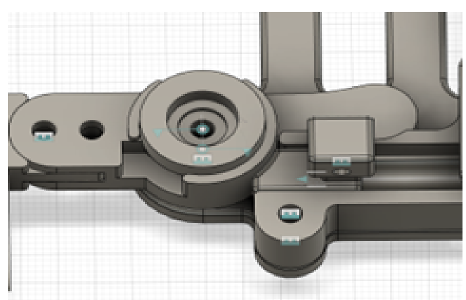

(b) Locking Mechanism (Unlock)

Figure 10: Locking Mechanism

1. **Switchblade Structure**: This structure is mainly achieved through a torsion spring with an outer diameter of 10 mm, a wire diameter of 1.4 mm, and 6 coils. The torsion spring keeps the wings unfolded in its natural state, and the locking structure ensures that the wings are locked in place when unfolded (see Figure 9(a)). When a slider is inserted, the spring is compressed, causing the wings to fold parallel to the body (see Figure 9(b)). When the slider is removed, the wings will return to the unfolded state under the action of the spring. In addition to the spring, the switchblade structure also consists of a trigger and a fixing structure. The trigger is mainly composed of three main parts, with the longer end in contact with the slider. Folding function is achieved by inserting and removing the slider. The middle circular part is connected to the spring to achieve the rebound effect, and the feet of the spring are embedded in the groove of the trigger to achieve the connection. At the same time, the upper and lower sides of this part are connected to the body through flat thrust bearings (outer diameter 21mm, inner diameter 12 mm, thickness 5 mm). In addition, the middle part also has a 10mm wide groove connected to the locking structure. The shorter end is connected to the wing through two M4 screws. The fixing structure is mainly composed of two upper and lower plates. The upper plate is connected to the trigger through M4 screws and flat bearings. The lower plate is connected to the trigger through M4 screws and flat bearings, and also has a groove for fixing the spring. The fixing structure and trigger are both made by 3D printing using PLA material.

2. **Locking Mechanism**: The locking mechanism is mainly composed of a fixed structure, a spring (wire diameter of 0.4 mm, outer diameter of 8 mm, and length of 25 mm), and a small slider. The small slider and spring are located inside the fixed structure. When the wing is in the deployed state, the small slider will be inserted into the groove of the trigger structure under the action of the spring, thus locking the wing (see Figure 10(a)). When folding the wing, first manually pull the slider backwards, and then fold the wing (see Figure 10(b)). The fixed structure is mainly composed of two parts, upper and lower. The spring is fixed in a cylindrical groove and can be horizontally compressed and stretched along the groove. The slider follows the spring to move forward. The cylindrical protrusion at the upper end of the slider can be inserted into the square groove on the bottom plate of the fixed structure. The handle can be connected to the slider to make manual pulling more comfortable and also serves as a certain limiting function. Structure in this part are 3D printing using PLA.

3. **Wings**: There are three sets of wings in this subsystem: the front wing, tail wing, and vertical tail fin. The front wing and tail wing have the same shape, width, and length, with a cross-sectional view of the wing. The width of the front wing and tail wing is 40 mm, the length is 150 mm, and the thickest part is 7 mm. The front wing and tail wing mainly provide lift for the drone. They are connected to the trigger of the switchblade structure through an M4 screw. When the drone is on the electromagnetic launcher, the wings are folded parallel to the fuselage. When the trigger is released after the drone leaves the launcher, the wings rotate 90

degrees to become perpendicular to the fuselage and are locked in place by a locking structure to ensure flight stability. The vertical tail fin is connected to the trigger of the switchblade structure through an M4 screw. The length of the vertical tail fin is 52 mm, the widest part is 30 mm, and the narrowest part is 15mm. All three pairs of wings are made of PLA material using 3D printing.

2.3.2 Design Alternatives

As our launcher subsystem did not provide enough acceleration as we expected. We design a much lighter switchblade drone as shown in Figure 11(a) and 11(b). This drone can achieve most functions except providing a space for the flight control system. In this way this drone is an alternative without power and flight control. It can be used to test our launcher. The design of the new switchblade structure is shown in Figure 12(a) and 12(b). This structure can rotate 90 degree. After rotating is over, the locking mechanism will lock the rotation and keep the wing stable while flying. To fold the wing after locking, the button on the structure need to be press. Then the whole structure is unlocked and can be rotated again. The alternative weighs 40 grams while the original design weighs 800 grams (including flight control).

(a) In Open Mode (b) In Fold Mode

Figure 11: Overview of the Alternative

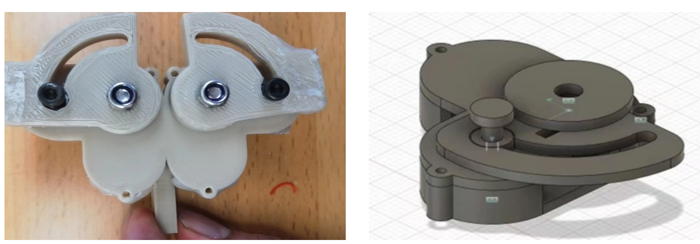

(a) Real Product (b) CAD Design

Figure 12: New Switchblade Structure

2.4 Flight Control Subsystem

2.4.1 Design Description & Justification

The flight control subsystem consists of a remote-control unit, a receiver, an on-board battery, two steering engines and a ducted fan. The diagram of this subsystem is shown in Figure 13. The remote-control unit will use an antenna to send our instructions of turning, the remote signal will then be receive and interpret by the on-board receiver which is also equipped with an antenna. The speed control will then produce signal to control the action of the steering engine and the motor in the ducted fan, thus, to produce thrust and achieve turning. An on-board battery will be implemented to provide power for the engine. The aim of this subsystem is helping the drone to fly a desired distance and control its direction in real time.

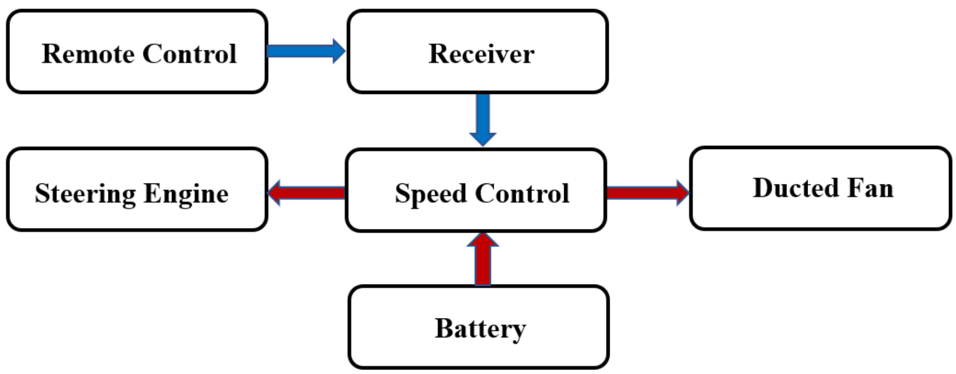

Figure 13: Subsystem Diagram of Flight Control Subsystem

We need following key components:

1. **Speed Controller**: Inside our control panel there is also an electronic speed controller. It is implemented between the power supply and the engines, used to control the speed of the motor and the move of steering engines. According to our desired motor, the speed controller we select is a brush electronic speed controller, and it can be attached straightly to a lithium battery. Our choice is Hobbywing V2 Speed Controller, it has 40 A working current, 55 A instant current, 5 V working voltage and weight of 39 g.

2. **Remote Control**: Our choice for the remote control and its corresponding receiver is Microzone MC6C Control and MC7RB Receive. They have frequency band of 2.400 GHz to 2.483 GHz.

3. **Steering Engine**: Our choice for steering engine is Micro servo MG90S, it is 90 degrees movable, 12 g in weight, 4.8 V working voltage and 2 kg/cm torque.

4. **Ducted Fan**: Our choice for motor and propeller is Powerfun 3S 4900 kV. It has 11 blades, the length of 76.0 mm, the diameter of 63.0 mm and the weight of 77 g. The

motor has 478 W maximum power, 38A maximum current and 12.6 V maximum voltage.

5. **Battery**: Our choice for battery is JFLY 3S Lithium Battery. It has capacity of 1500 mAh.

When assembling the flight control components on the drone, we did detailed calculations toward where to put each component, in order to distribute the weight evenly on the drone, thus, to make sure the result drone will not lose its balance when flying. Regarding how to precisely manipulate the two ailerons using our steering engines, we implemented two transmission rods and two sets of adapting pieces. Finally, our assembled flight control system is shown in Figure 14.

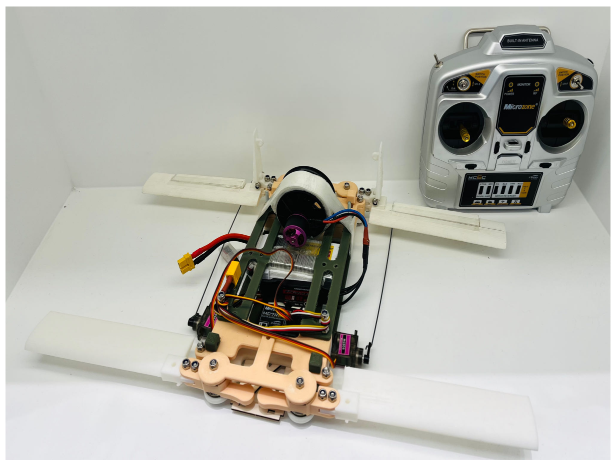

Figure 14: Assembled Flight Control Subsystem

2.4.2 Design Alternatives

For the flight control subsystem, we originally had three plans, one is using a vector motor that can provide thrust from a different direction, one is a traditional motor and steering engine system, the other is a match of a ducted fan with steering engines. The vector motor method is basically a large integrated structure at the head or the bottom of the drone, it has the pros of easy implementation and a more flexible angle of the driving force. While its disadvantages include high cost, hard to repair, and easy to break, most importantly, attaching such a big structure might cause the drone to lose its balance. The typical motor and steering engine method, however, has advantages like low cost and disperse weight. While it also has problems of lack of thrust and need for multiple wires on the drone's body. Lastly, ducted is just an improved version of traditional motor and propeller, it provides bigger thrust while having a larger weight. After carefully analyzing and discussing with the professor, we chose the ducted fan and steering engine method, as it will help maintain the balance of the drone, while providing a relatively bigger thrust.

3 Requirements and Verification

3.1 DC Power Supply Subsystem

3.1.1 Requirements

1. The output voltage must be a stable 450 V DC, maintained for at least one minute.
2. The power supply subsystem should be capable of storing energy in a 450 V 1000 μF capacitor.
3. The temperature of subsystem components, particularly the coils, must not exceed 200 degrees Celsius to avoid fire, short circuits, breakage, and other hazards.

3.1.2 Verification

1. Utilize the integrated voltmeter to confirm the output voltage is 450 V and maintains a stable DC level on both sides of the output.
2. Connect a depleted capacitor to the power supply subsystem's output and verify if the capacitor has stored energy after one minute of charging.
3. Operate the subsystem for 50 seconds and use a temperature measuring gun to monitor the temperature change of its components, especially the coil, over time. Ensure the maximum temperature does not surpass 200 degrees Celsius.

3.1.3 Quantitative Results

1. Using the voltmeter reading, we can adjust the desired output voltage by manipulating the sliding resistor.
2. As indicated by the charging circuit's LED, the capacitor can complete charging within 30 seconds.
3. Under the temperature measuring gun's monitoring, none of the components' temperature exceeds 200 degrees Celsius, and no hazards such as short circuits were detected in multiple tests.

3.2 Electromagnetic Accelerator Subsystem

3.2.1 Requirements

1. The drone should accelerate continuously and finally gets a speed of 3-6 m/s to take off.
2. The launch system can work outside normally when the wind speed is 0-3 m/s.
3. The coils need to be connected one by one when the cart is forwarding.

3.2.2 Verification

1. Use high-speed camera to record the whole process when testing. Calculate the average speed when the cart is at different positions.
2. Use wind tunnel to create working situations with different wind speeds. Do the speed test same as the above and observe if the system is stable.
3. Observe that if the blue light on photoresistance flashes.

3.2.3 Quantitative Results

1. The drone can only achieve about 1 m/s with the help of rubber band. The main reason is that there must be some distance from the coils and the cart in order to avoid the collision between photoresistances and the cart. The electromagnetic force decreases sharply when the distance increases. What's more, the resulting electromagnetic force, which has a large lateral component, does not accelerate the cart but creates more friction.
2. The launch system works and has a similar result.
3. The flash of blue light is observed and there are some small voice to prove that the coil is working.

3.3 Switchblade Drone Subsystem

3.3.1 Requirements

1. Drone can fold the wing when in the launcher and open the wing when leave the launcher.
2. Drone can fix its wing after the wing is open.

3.3.2 Verification

1. Test the switchblade structure with and without launcher.
2. Exerting force on the wing to test if the locking mechanism is working.

3.3.3 Quantitative Results

1. The switchblade function is achieved with or without launcher.
2. After exerting 400 g weight on the open wing. The wing doesn't blend or fail.

3.4 Flight Control Subsystem

3.4.1 Requirements

1. On-board components should be light enough, no more than 500 g.
2. The design of the steering engine system allow drone to turn its direction efficiently.
3. Each component should work within its voltage and current limit. For example: $V(steeringengine) \leq 4.8$ V, $V(speedcontroller) \leq 5$ V.

3.4.2 Verification

1. Sum up the total weight, if more than limit, find better components to substitute the old ones.
2. Use prototype drone (similar shape and weight but no detailed mechanism) to test the navigate function.
3. Simulate the system on computer to check the circuit work properly. Integrate the system step by step , use a multi-meter to measure the parameters and ensure the safety before connecting a new component.

3.4.3 Results

1. The total weight of our final on-board components is 291.1 g, which satisfy our requirement.
2. The steering engine and aileron system works well on our dummy planes, it enable the plane to turns its direction smoothly without rollover.
3. During the process of assembling, we careful exam each step and there was no incident happen, every components were able to work within their permitted conditions.

4 Cost and Schedule

4.1 Cost

4.1.1 Labor

We take the average first year salary of UIUC graduates as our hourly wage. Our working hours is 18 hours per week before may, and for the last three weeks, we work around 30 hours per week. For this project, we work 13 full weeks, so the overall average working hour would be 20.77 hours. Then we can get following labor cost table, the resulting total labor cost would be around $ 54000. Table 1 shows the costs of labor.

Table 1: Costs of Labor

Name	$/Hour	Hours/Week	Weeks	Multiplier	Cost ($)
Shuyang	20	20.77	13	2.5	13500
Zheng	20	20.77	13	2.5	13500
Xinyu	20	20.77	13	2.5	13500
Ruike	20	20.77	13	2.5	13500
Total	20	83.08	13	2.5	54000

4.1.2 Parts

For the components and materials, see the following bill of materials (BOM). The resulting expected cost of the parts is 415.3$. Table 2 shows the bill of materials.

Table 2: Bill of Materials

Name	Company	Description	Cost ($)	Qty	Total($)
3S 4900KV Ducted Fan	Powerfun	12.6 V, 38 A, 478 W, 77 g	18	1	18
MG90S Steering Engine	Micro servo	90 degrees, 12 g, 4.8 V, 2 kg/cm	2.5	2	5
3S Lithium Battery	JFLY	1500 mAH, 11.1 V	10.5	1	10.5
V2 Speed Controller	Hobbywing	40 A, 55 A(instant), 5 V, 39 g	12	1	12
B3 Charger	imaxRC	10 W, 800 mA	3	1	3
MC6C Control	Microzone	70 MW, 6 V, 550 g	18	1	18
MC7RB Receive	Microzone	6 V, 9.6 g	4	1	4
Launcher PCB Board	Self-Designed	Details in subsystem part	100	2	200
ZVS Module	Self-Designed	Details in subsystem part	12	2	24
Aluminum Rail	Oulihua	50*150*100 0mm	17.4	1	17.4
PLA	ELEGOO	1000 g	9.3	2	18.6
PMMA Board		300 g	20	4	80
Spring		304	0.8	6	4.8
Total					415.3

4.1.3 Grand Total

Except from labor and components cost, we used varies instruments and machines provided by school's lab, here we include the estimated fee of processing and incidental expenses:

1. Estimated 3D printing fee: $ 15
2. Estimated laser cutting fee: $ 12
3. Processing instruments expense: $ 13.2

So the grand total would be: $54000[Labor] + 415.3[Parts] + 15 + 12 + 13.2 = \$\ 54455.5$

4.2 Schedule

Table 3 shows the schedule for our group.

Table 3: Schedule

Date	Shuyang	Zheng	Xinyu	Ruike	Overall
2/20	Search information, preparation	Search information, preparation	Search information, preparation	Search information, preparation	Background research, preparation
2/27	Pre-design of launcher mechanism	Pre-design of launcher circuit	Pre-design of drone mechanism	Pre-design of flight control	Identify solutions, allocate tasks
3/06	Design and analysis of launcher mechanism	Design and analysis of launcher circuit	Design and analysis of drone mechanism	Planning of flight control, help with launcher part	Focusing on the launcher part, math analysis
3/13	Design and analysis of launcher mechanism	Test and analysis the launcher circuit	Design and analysis of drone mechanism	Design and analysis the flight control, help with launcher part	Focusing on the launcher part, start to look for material and components
3/20	Model and print launcher mechanism	Test and analysis the launcher circuit	Model and print drone mechanism	Design and analysis the flight control	Finalize launcher part, start to print mechanism

Continued on next page

Table 3: Schedule (Continued)

3/27	Model and print launcher mechanism	Build and check the launcher circuit	Model and print drone mechanism	Design and analysis the flight control	Build launcher part, print mechanism
4/03	Finalize the launcher mechanism	Finalize the launcher circuit	Finalize the Drone mechanism	Finalize the launcher circuit	Finalize the launcher drone system
4/10	Integrate and test the launcher drone part	Integrate and test the launcher drone part	Integrate and test the launcher drone part	Build and test of the flight control part	Test launcher drone part, implement flight control
4/17	Integrate and test the launcher drone part	Finalize and improve flight control	Integrate and test the launcher drone part	Finalize and improve flight control	Test launcher drone part, finalize flight control
4/24	Integrate and test the whole system	Integrate and test the whole system	Integrate and test the whole system	Integrate and test the whole system	Integrate and test the whole system
5/01	Integrate and test the whole system	Integrate and test the whole system	Integrate and test the whole system	Integrate and test the whole system	Integrate and test the whole system
5/08	Modify and improve the system	Modify and improve the system	Modify and improve the system	Modify and improve the system	Modify and improve the system
5/15	Modify and improve the system, prepare for the demo	Modify and improve the system, prepare for the demo	Modify and improve the system, prepare for the demo	Modify and improve the system, prepare for the demo	Modify and improve the system, prepare for the demo

5 Conclusion

5.1 Accomplishments

The project successfully meets most of the high level requirements. The launch system can accelerate the drone continuously and let the switchblade drone deploy the wings and take off. Also, the flight control system is applied to the drone. Nevertheless, the system fails to accelerate the drone to 3-6 m/s.

5.2 Uncertainties

The main uncertainty for the project is that the launch system cannot offer big enough electromagnetic force as expected. According to the Biot Savart's law is shown in Equation 15:

$$\overrightarrow{\mathrm{B}} = \int \mathrm{d}\overrightarrow{\mathrm{B}} = \int \frac{\mu_0}{4\pi} \frac{\mathrm{Id} \times \overrightarrow{\mathrm{r}}}{\mathrm{r}^3} \tag{15}$$

It is found that the distance plays a much significant role when generating the magnet field. When we did the tolerance analysis experiment to estimate the final speed of drone, we accelerate the magnet which clings to the coils. However, when we are accelerating the drone, we have to leave a space of about 10mm. Assuming the distance from the magnet to the coil in the experiment is 1 mm, the resulting magnetic induction varies by a factor of 100 which leads to a 100 times difference in the electromagnetic force. Moreover, some safety accidents happened during the project. Therefore, we decrease the working voltage from 450 V to 200 V when testing. This also greatly affects the acceleration effect.

5.3 Future Work / Alternatives

1. A new way to trigger photoresistances should be came up with in order to minimize the distance from the cart and the coils. It can greatly improve the performance.

2. Capacity banks with larger capacity should be employed. Extremely high voltage can lead to danger, so we should try to increase the capacity which can also offer more energy to accelerate better.

3. Voltmeter and ammeter should be attached to each coil. Monitoring voltage and current in real time can ensure that safety incidents do not occur.

4. Lighter drones and flight control systems need to be came up with in order to improve the speed of the drone with similar launch system.

5.4 Ethical Considerations

According to the IEEE Code of Ethics [5], as professionals, we hold paramount the safety, health, and welfare of the public and are responsible for promptly disclosing factors that may endanger the public or the environment. Therefore, when testing our electromagnetic launch system and switchable drone, we will take precautions to ensure public safety. Warning signs will be placed around the test sites to prevent unauthorized entry to potentially dangerous areas.

Furthermore, in accordance with the IEEE Code of Ethics [5], we will avoid any unlawful conduct in our professional activities, specifically relating to laws and regulations regarding unmanned aerial vehicles. Compliance with all regulations and laws is essential to ensure the safety of the public and the environment. According to the Chinese agency responsible for drone safety[6], CAAC, drone use is allowed without a permit or a license in China, subject to UAS Laws, the general rules for flying drones in China. The restrictions include maximum height (120 meters), maximum distance (must keep the drone in sight). We will obey the rules strictly and apply for permission if necessary.

Lastly, we will seek, accept, and offer honest criticism of technical work, acknowledging and correcting errors, in line with the IEEE Code of Ethics [5]. We will actively seek guidance and constructive criticism from peers and experts to optimize our project and ensure the highest level of technical excellence.

When utilizing our electromagnetic launch system, the power supply system generates high voltage and an extremely high current flows through the coil, both of which can be lethal to the human body. Therefore, we decide to design a voltage boost module to ensure that we can use a relatively low voltage power supply to improve its safety. Additionally, the large current flow may generate significant heat at both the power supply and the coil, potentially damaging the circuit or causing a fire. Hence, we decide to install some cooling devices to make sure the temperature doesn't get too high.

According to the Occupational Safety and Health Administration (OSHA) standards[7], employers should provide a safe and healthy workplace, free from recognized hazards that could cause harm to employees. So we should ensure that appropriate safety measures, such as warning signs, are in place to alert people of potential hazards. OSHA standards also require that employers conduct regular inspections. So we should ensure that the whole system is in good working condition and that all safety measures are functioning properly.

According to Electromagnetic Compatibility (EMC) regulation[8], an electrical and electronic equipment should permit it to operate as intended in the presence of other electrical and electronic equipment, and not to adversely interfere with that other equipment. So we will check and make sure that the launch system does not have a negative influence on surrounding electrical and electronic equipment. Therefore, we will exercise caution and implement appropriate safety measures during testing to ensure the safety of all individuals involved.

6 References

[1] AeroVironment, “Switchblade Tactical Missile System,” *AeroVironment*, 2021. [Online]. Available: https://www.avinc.com/tms. [Accessed: 02-Mar-2023].

[2] J. Zhu, C. Zhang, H. Xie, and J. Zhan, “Research progress in electromagnetic launch technology,” *Journal of Physics: Conference Series*, vol. 1577, no. 1, p. 012008, 2020.

[3] S. Alamri, A. Khaligh, “Design, Development, and Control of an Electromagnetic Launch System for Small Fixed-Wing Unmanned Aerial Vehicles,” *IEEE Transactions on Transportation Electrification*, vol. 5, no. 2, pp. 734-744, 2019.

[4] Q. Xin, W. Cao, C. Shang, W. Liu, “Study on Energy Conversion Efficiency of a Single Stage Induction Coiler,” *Journal of Naval Aviation University*, vol.26, no.3, pp.331-336, 2011.

[5] Ieee.org, “IEEE code of Ethics,” IEEE. [Online]. Available: https://www.ieee.org/about/corporate/governance/p7-8.html. [Accessed: 02-Mar 2023].

[6] M. at D. Laws, “Drone laws in China,” Drone Laws. [Online]. Available: https://drone-laws.com/drone-laws-in-china [Accessed: 19-Mar 2023].

[7] Osha.gov, “Occupational Safety and Health Administration” United States Department of Labor. [Online]. Available: https://www.osha.gov/electrical/standards. [Accessed: 19-Mar 2023].

[8] Etsi.org, “Electro Magnetic Compatibility” ETSI. [Online]. Available: https://www.etsi.org/technologies/emc. [Accessed: 19-Mar 2023].